Data Supplement.

Supplemental Figures

Supplemental Figure 1. FAT1 immunofluorescence in the five additional cases of FAT1-associated DNMN demonstrating granular mesangial and capillary loop staining. Note that granular staining along the glomerular capillary loops is either global or segmental. FAT1 was negative within glomeruli in PLA2R-positive MN controls. Scale bars for all images = 20 µm.

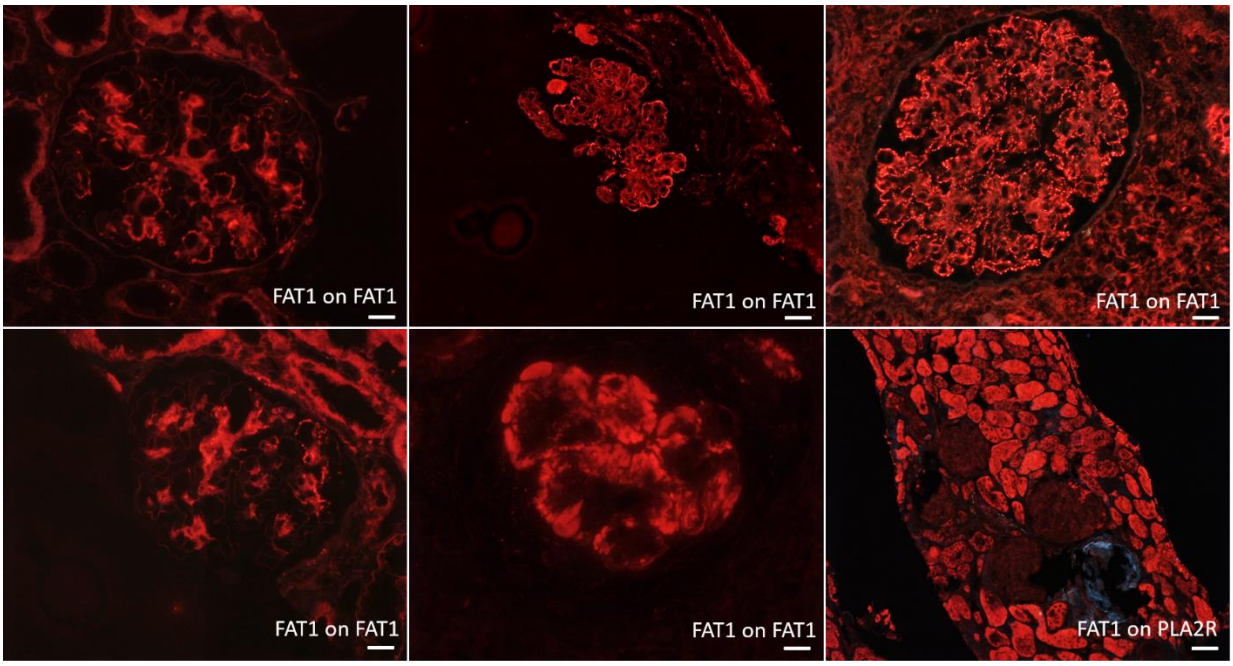

Supplemental Figure 2. Representative case of FAT1 associated membranous nephropathy in a patient with both antibody-mediated and cellular rejection. A) Jones methenamine silver stain demonstrating a representative glomerulus demonstrating small holes along the capillary loops; B) IgG immunofluorescence demonstrating granular capillary loop staining in a glomerulus; C) Paraffin immunofluorescence for FAT1 shows a similar pattern to IgG staining within glomeruli; D) H & E stain showing plasma cell-rich interstitial inflammation and edema; E) PAS stain showing severe lymphocytic tubulitis; F) Intimal arteritis and chronic transplant arteriopathy; G) H & E stain demonstrating acute tubular injury; H) H & E stain showing peritubular capillaritis; I) C4d immunohistochemistry demonstrates positivity along peritubular capillaries. All scale bars = 20 µm.

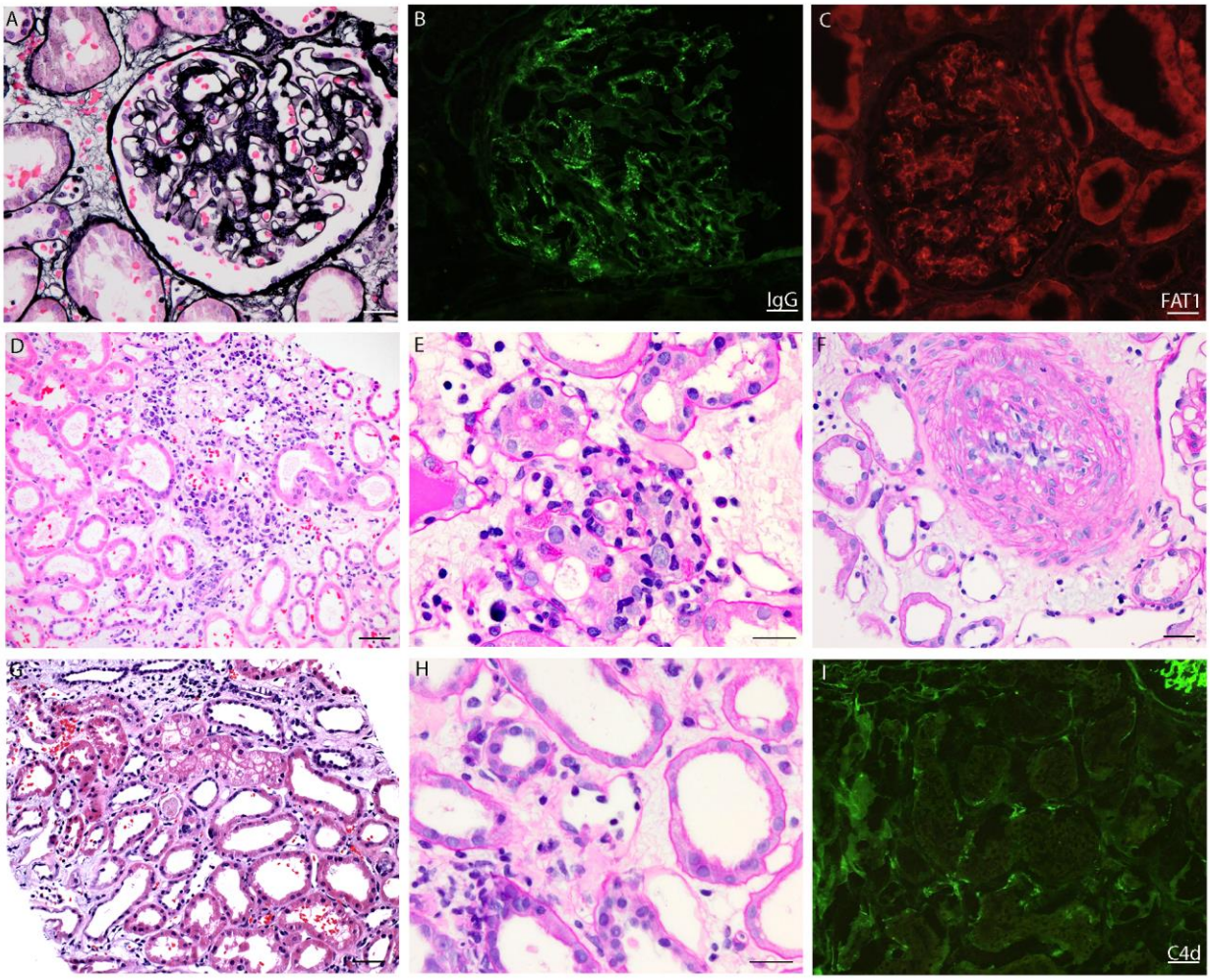

Supplemental Figure 3. Histopathology of a typical case of recurrent PLA2R-positive membranous nephropathy. A) Mason-Trichrome stain demonstrating no significant fibrosis or inflammation, Scale bar = 500 µm.; B) PAS-stain showing a normocellular glomerulus with mildly prominent capillary loops, Scale bar = 20 µm; C) Ultrastructural photomicrograph showing stage I subepithelial electron dense deposits; D) Immunofluorescence for IgG showing a global granular capillary loop pattern of staining, Scale bar = 20 µm; E) Immunofluorescence for C3 is of similar intensity, Scale bar = 20 µm; F) Positive immunohistochemistry for PLA2R is seen along the glomerular capillary loops. Scale bar = 20 µm.

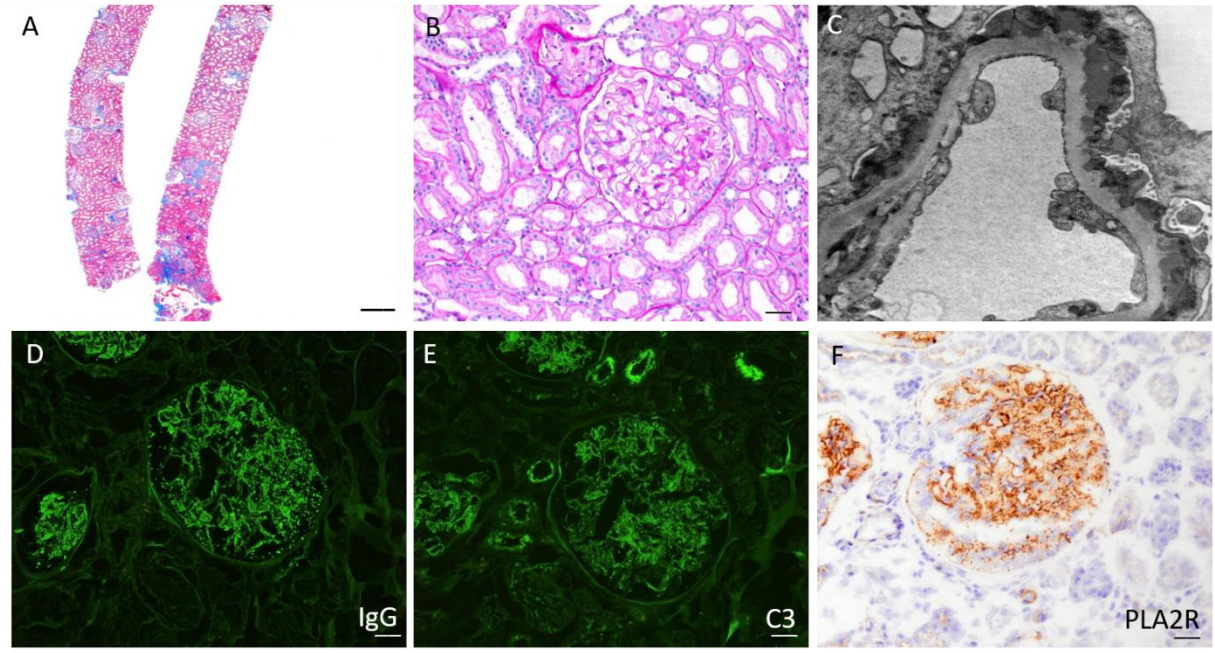

Supplemental Figure 4. Immunofluorescence for HLA DQ was negative within podocytes or along the capillary loops in all FAT1 positive cases. Scale bars for all images = 20 µm.

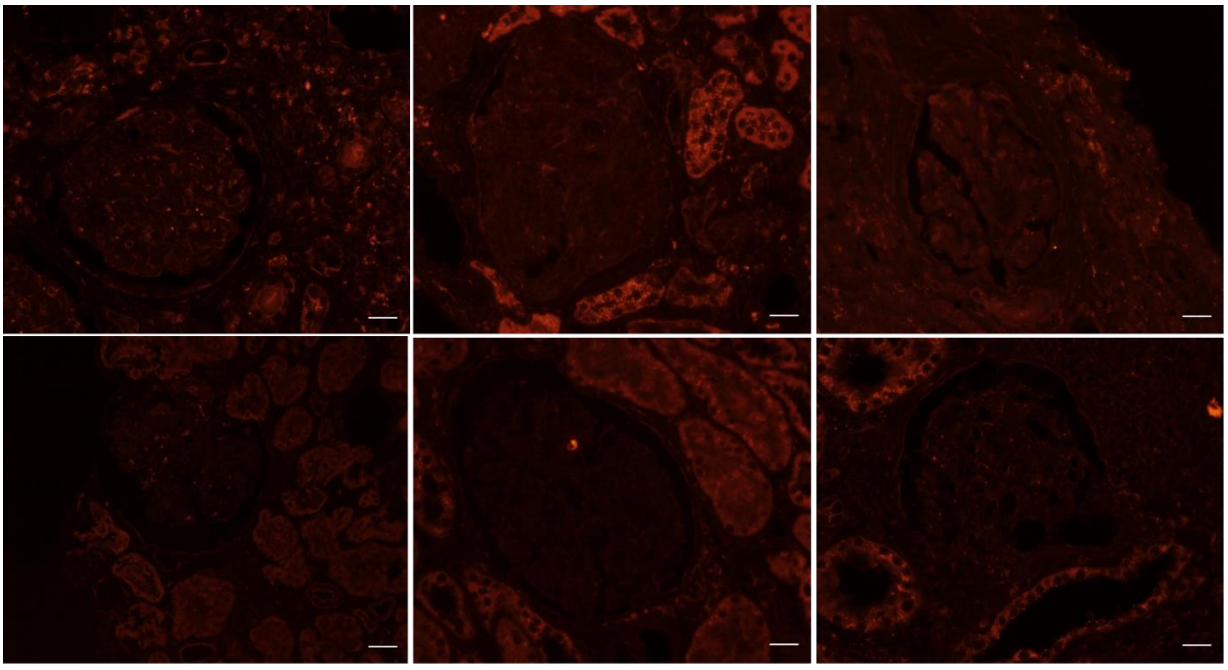

Supplemental Figure 5. FAT1 staining is negative along the glomerular capillary loops within cases of (A) PLA2R, (B) THSD7A, (C) NELL1, and (D) EXT1-associated MN, demonstrating specificity of staining. Scale bars for all images = 20 µm.

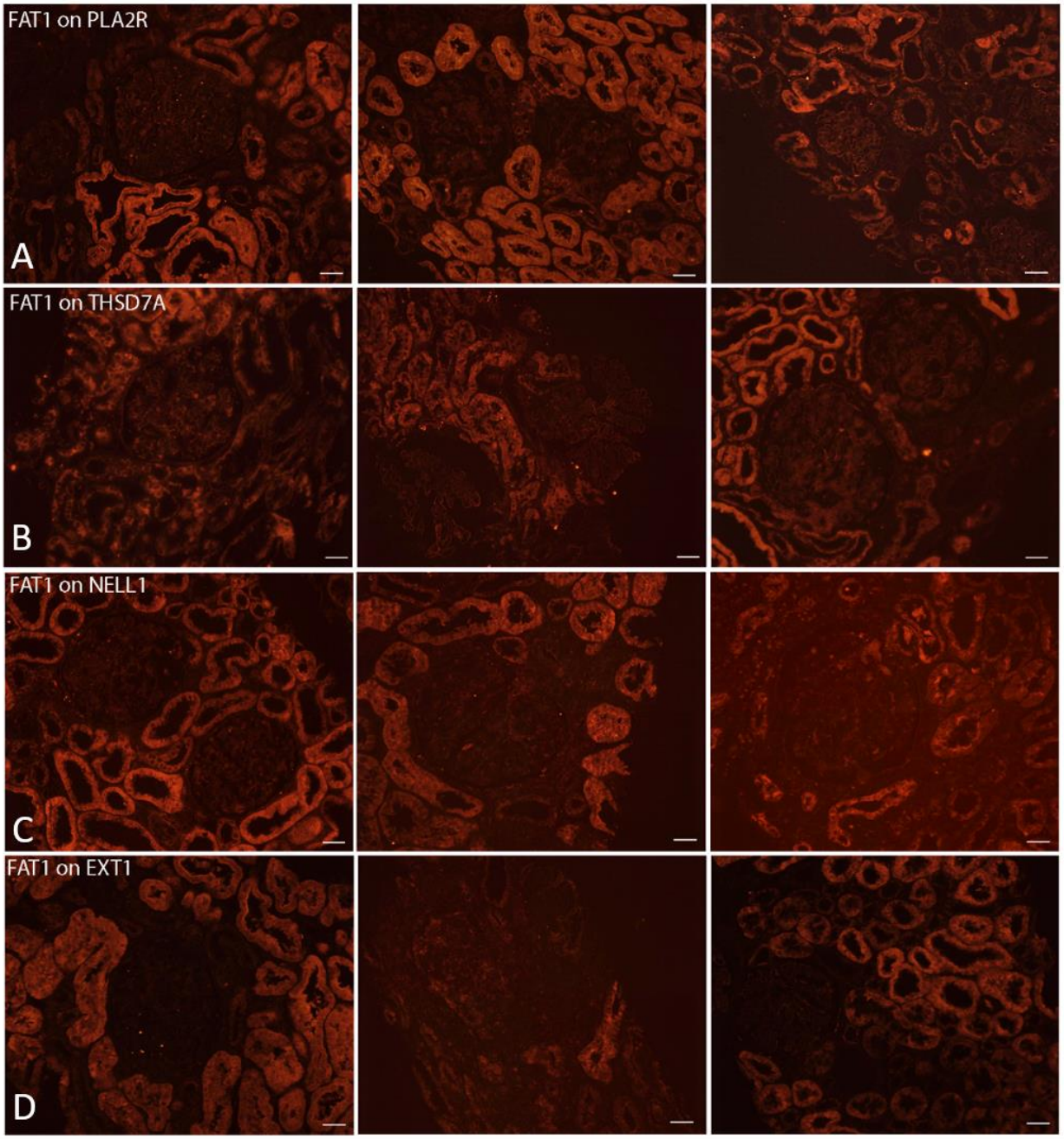

Supplemental Figure 6. FAT1 Immunohistochemistry. A) In FAT1 negative cases, FAT1 immunostaining is restricted to podocytes. B) In FAT1 positive cases, there is granular staining present along the glomerular capillary loops in addition to podocyte staining. Scale bars = 20 µm.

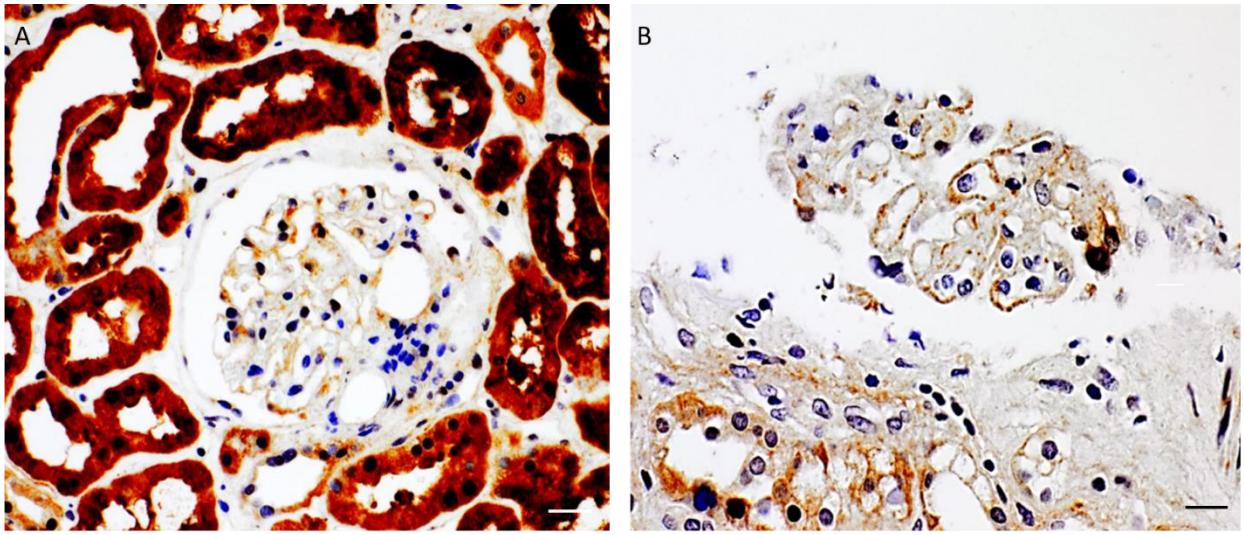

Supplemental Figure 7. Mass spectrometry confirms protocadherin FAT1 is an antigen in MN through an independent technique than previously reported. A) Volcano plot of protein G immunoprecipitation of immune complexes recovered from residual frozen biopsy tissue reveals FAT1 highly enriched in immune complexes. B) Peptide map demonstrating multiple FAT1-specific peptides enriched in the case in (A).

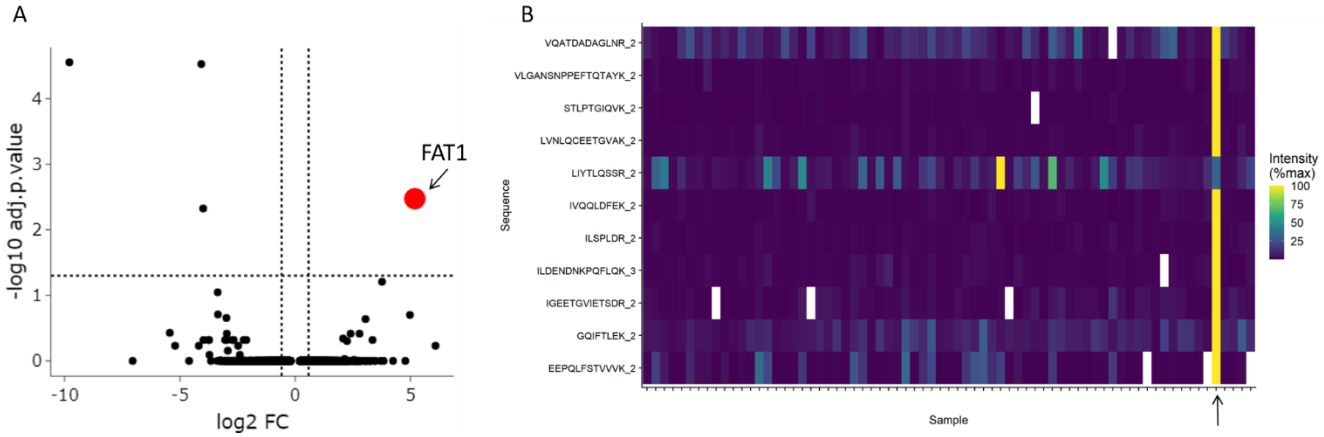

Supplemental Table 1. Histopathologic characteristics of MN cases in renal allografts in the presence or absence of allograft rejection.

Parameter	No rejection	Total rejection	Antibody mediated	T-cell mediated	Borderline TCMR	Vascular rejection	Mixed rejection	FAT1
n=	174 (50.1% total)	173 (49.9% total)	53 (30.6% rejection)	12 (6.9% rejection)	21 (12.1% rejection)	3 (1.7% rejection)	84 (48.6% rejection)	11 (from 6 patients)
Immunofluorescence and antigen status								
IgA pos 0	21.8% 136/174	19.0% 140/173	22.6% 41/53	25.0% 10/12	19.0% 16/21	33.3% 2/3	15.5% 71/84	36.4% 7/11

1+	27/174	21/173	7/53	2/12	4/21	1/3	7/84	3/11
2+	10/174	10/173	4/53	0/12	0/21	0/3	6/84	1/11
3+	1/174	2/173	1/53	0/12	1/21	0/3	0/84	0/11
IgG pos	94.8%	94.3%	96.2%	100%	100%	100%	96.4%	100%
0	6/174	9/173	6/53	0/12	0/21	0/3	3/84	0/11
1+	26/174	25/173	6/53	0/12	5/21	0/3	14/84	3/11
2+	54/174	45/173	18/53	3/12	1/21	0/3	23/84	5/11
3+	88/174	94/173	23/53	9/12	15/21	3/3	44/84	3/11
IgM pos	28.2%	27.6%	32.1%	25.0%	19.0%	33.3%	27.4%	18.2%
0	125/174	125/173	36/53	9/12	17/21	2/3	61/84	9/11
1+	33/174	29/173	9/53	3/12	1/21	0/3	16/84	0/11
2+	14/174	15/173	7/53	0/12	3/21	0/3	5/84	1/11
3+	2/174	4/173	1/53	0/12	0/21	1/3	2/84	1/11
C3 pos	60.3%	55.2%	47.2%	58.3%	76.2%	66.7%	52.4%	45.5%
0	67/174	77/173	26/53	4/12	5/21	1/3	40/84	6/11
1+	27/174	65/173	17/53	5/12	9/21	1/3	34/84	5/11
2+	27/174	24/173	10/53	2/12	3/21	1/3	8/84	0/11
3+	6/174	7/173	0/53	1/12	4/21	0/3	2/84	0/11
C1q pos	12.6%	16.1%	17.0%	8.3%	4.8%	33.3%	19.0%	54.5%
0	152/174	145/173	44/53	11/12	20/21	2/3	68/84	6/11
1+	9/174	14/173	5/53	0/12	0/21	0/3	9/84	3/11
2+	10/174	10/173	2/53	0/12	1/21	1/3	6/84	1/11
3+	3/174	4/173	2/53	1/12	0/21	0/3	1/84	1/11
PLA2R	50.4%	30.3%	27.9%	58.3%	50.0%	33.3%	21.7%	0%
	69/137	44/145	12/43	7/12	9/18	1/3	15/69	0/11

Supplemental Methods.

Patient cohorts. Kidney biopsies were screened for FAT1 positivity from two institutions, The University of Utah in Salt Lake City and Arkana Laboratories in Little Rock, Arkansas. Human serum and/or biopsy specimens were obtained following institutional review board approval with waivers of consent at each study site. Clinical and pathologic information including demographics, DSA results, and kidney pathology reports from University of Utah patients were obtained from ARUP or Arkana laboratories for further review. Renal tissue samples from patients diagnosed with DNMN (all PLA2R negative) with no clinical history or histologic features of lupus were had FAT1 immunostaining performed at Arkana Laboratories. A total of six cases of FAT1 positive DNMN were included, three from the University of Utah and three from Arkana Laboratories. DNMN was defined as development of MN in the renal allograft in patients without a history of ESKD due to MN or a positive anti-PLA2R serology prior to transplantation. Donor kidney biopsies, pre-implantation, or post-perfusion kidney biopsies were not available in any of the cases. However, given the low incidence of MN among the general population, it would be highly unusual for these cases to represent *de novo* disease.

Immunofluorescence for FAT1. FAT1 staining was performed by paraffin immunofluorescence as follows. Formalin fixed paraffin embedded tissue sections, freshly cut at 3 μm, were deparaffinized, and antigen retrieval was performed by incubation at 99°C in Tris/EDTA high pH buffer (pH 9.0, Agilent Technologies). The sections were incubated with rabbit polyclonal anti-FAT1 antibody (1:100, AbCam; ab198892) for 40 minutes, washed in phosphate buffered saline, and then reacted with

Rhodamine Red-X AffiniPure Goat Anti-Rabbit IgG as a secondary antibody at 1:100 dilution, which was solid-phase adsorbed to ensure minimal cross reaction with human IgG (1:100; Jackson Immunoresearch). Sections were washed in 3 times in phosphate buffered saline and coverslipped in aqueous mounting medium. Slides were evaluated by standard immunofluorescence microscopy and cases were categorized as positive with granular capillary loop staining in the glomeruli of 1+ or greater immunofluorescence intensity and negative if without capillary loop staining (staining within podocytes alone may be present as FAT1 is expressed within podocytes).

Negative controls were performed to ensure antibody specificity through staining five cases each of other antigen types (PLA2R, THSD7A, EXT1, and NELL1-positive MN), as well as other proteinuric disease states (fibrillary glomerulopathy, minimal change disease, primary focal segmental glomerulosclerosis, and diabetic nephropathy). For identification of control MN cases, immunofluorescence was performed for PLA2R (PLA2R rabbit polyclonal antibody, catalog number HPA012657; Sigma), THSD7A (THSD7A mouse polyclonal antibody, catalog number AMAB91234; Atlas Antibodies), and EXT1 (EXT1 rabbit polyclonal antibody, catalog number PA5-60699; Invitrogen). Following incubation with primary antibodies for 40 minutes at room temperature, slides were washed 3 times with phosphate buffered saline, followed by incubation with a secondary antibody. Secondary antibodies included FITC-conjugated goat anti-mouse IgG (Jackson Immunoresearch, catalog number 111-095-003) for mouse primaries or Rhodamine Red X Affinipure goat anti-rabbit IgG (Jackson Immunoresearch, catalog number 111-295-444) for rabbit primaries. Slides were incubated with secondary antibody in the dark for 30 minutes at room temperature, followed by washing three times with phosphate buffered saline, and coverslipping using aqueous mounting medium. Slides were evaluated by standard immunofluorescence and granular capillary loop staining of 1+ or greater intensity was considered a positive result.

HLA-DQA1 staining was performed using HLA-DQ rabbit polyclonal antibody (catalog number PA5-5292; Thermo-Fisher Scientific) at 1:100 dilution, following antigen retrieval by incubation at 99°C in high pH Tris/EDTA buffer (pH 9.0, Agilent Technologies). Sections were stained for 40 minutes at room temperature, followed by washing 3 times in phosphate buffered saline. Rhodamine Red-X AffiniPure Goat Anti-Rabbit IgG was added as a secondary antibody at 1:100 dilution, incubated for 40 minutes at room temperature in the dark, followed by washing with phosphate buffered saline and coverslipping using aqueous mounting medium. Human tonsil tissue was used as a positive control, which demonstrates positivity within germinal centers.

Immunohistochemistry**:** FAT1 was detected in human kidney tissue by immunohistochemistry with peroxidase-based detection. Freshly cut 3 um tissue sections were deparaffinized and heated to 99°C for 15 minutes in high pH buffer for antigen retrieval. Tissue sections were incubated with mouse anti-human FAT1 at 1:100 (AbCam, ab198892) for 40 minutes at room temperature, followed by washing in phosphate buffered saline and incubation with anti-mouse IgG-HRP as a secondary antibody (1:100, Jackson Immunoresearch) for 30 minutes at room temperature. Slides were washed, coverslipped, and evaluated by standard light microscopy. Staining in a granular capillary

loop distribution (1+ or greater) was considered a positive result, while staining within podocytes alone was considered FAT1-negative.

Protein G Immunoprecipitation: Protein lysates were prepared from kidney biopsy tissue frozen in optimized cutting medium, through washing biopsy cores in phosphate-buffered saline (PBS) four times, followed by disaggregation by bead-beating in 300 µl Pierce IP lysis buffer (Thermo-Fisher, Waltham MA, catalog #87787) with the addition of protease and phosphatase inhibitors (Halt protease and phosphatase inhibitor cocktail, Thermo-Fisher, catalog #78440). Immunoprecipitations were performed through addition of 50 µl of magnetic protein G Dynabeads (Thermo-Fisher, Waltham MA, catalog #1003D) and incubation at room temperature for 1 hour with shaking. Following incubation, beads were washed with PBS four times to reduce non-specific protein binding. After the final wash, the beads were frozen at -20°C until further analysis.

Mass Spectrometry: Peptides were produced through trypsin digestion of the immune complexes adhered to protein G beads post-immunoprecipitation.Data-independent acquisition mass spectrometry was used for analysis as follows. An UltiMate 3000 RSLC nano system (Thermo Scientific) was used to separate tryptic peptides on a 150 x 0.075 mm column packed with a reverse phase XSelect CSH C18 2.5 µm resin. The peptides were eluted with a gradient of buffer A (0.1% formic acid + 0.5% acetonitrile)/buffer B (0.1% formic acid + 99.9% acetonitrile), from a 97:3 ratio to a 60:40 ratio over 1 hour. Electrospray (2.25 kV) was used to ionize the eluted peptides on an Orbitrap Exploris 480 mass spectrometer (Thermo Scientific). Six gas-phase fractions of a pooled sample were acquired on the Orbitrap Exploris mass spectrometer with 4 m/z DIA spectra (30,000 resolution, normalized AGC target 100%, maximum inject time 66 ms) in a staggered window pattern to assemble a chromatogram library (S7). Precursor spectra were acquired after each DIA duty cycle, spanning the m/z range of the gas-phase fraction (i.e. 496-602 m/z, 596-702 m/z). For wide-window acquisitions, precursor spectra from each DIA cycle were acquired (385-1015 m/z, 60,000 resolution, normalized AGC target 100%, maximum injection time 50 ms), followed by 50x 12 m/z DIA spectra (12 m/z precursor isolation windows at 15,000 resolution, normalized AGC target 100%, maximum injection time 33 ms) using a staggered window pattern with optimized window placements. ScaffoldDIA (Proteome software) was used to configure DIA library searches. Gas-phase fractionated peptides were searched against a predicted spectral library by Prosit (S8), followed by searching wide-window acquisitions against the generated empirically corrected chromatogram library.

Statistical Methods: To summarize clinical data, given the small number of patients (n=6), we used the sample mean and standard deviations.

Supplemental references

S1. Al-Rabadi, L.F., et al., *Serine Protease HTRA1 as a Novel Target Antigen in Primary Membranous Nephropathy.* J Am Soc Nephrol, 2021. 32(7): p. 1666-1681.

S2. Caza, T.N., et al., *Discovery of seven novel putative antigens in membranous nephropathy and membranous lupus nephritis identified by mass spectrometry.* Kidney Int, 2023. 103(3): p. 593-606.

S3. Sethi, S., et al., *Neural epidermal growth factor-like 1 protein (NELL-1) associated membranous nephropathy.* Kidney Int, 2020. 97(1): p. 163-174.

S4. Sethi, S., et al., *Protocadherin 7-Associated Membranous Nephropathy.* J Am Soc Nephrol, 2021. 32(5): p. 1249-1261.

S5. Sethi, S., et al., *Exostosin 1/Exostosin 2-Associated Membranous Nephropathy.* J Am Soc Nephrol, 2019. 30(6): p. 1123-1136.

S6. Batal I, Vasilescu E-R, Dadhania DM, et al. *Association of HLA typing and alloimmunity with posttransplantation membranous nephropathy: a multicenter case series.* Am J Kidney Dis 2020 Sep; 76 (3): 374-383.

S7. Searle BC, Pino LK, Egertson JD, Ting YS, Lawrence RT, MacLean BX, et al. Chromatogram libraries improve peptide detection and quantification by data independent acquisition mass spectrometry. Nat Commun. 2018;9(1):5128.

S8. Gessulat S, Schmidt T, Zolg DP, Samaras P, Schnatbaum K, Zerweck J, et al. Prosit: proteome-wide prediction of peptide tandem mass spectra by deep learning. Nat Methods. 2019;16(6):509-18.